Ggraphene oxide loaded with nano-ZnO alters gut microbiota community to promote secondary bile acid synthesis and immunity response in fattening cattle

Haibo Zhang
Yichun University
Weikun Guan
Yichun University
Lizhi Li (jxlilizhi@qq.com)
Yichun University https://orcid.org/0000-0001-5709-0789
Dongsheng Guo
Yichun University
Qingfeng Xing
Yichun University
Chaoyong Huang
Yichun University
Chuanshuai Xiong
Yichun Teachers\' College: Yichun University
Baofeng Li
Yichun University
Ketian Chen
Yichun University
Cong Peng
Yichun University

Research Article

Keywords: Cattle, Graphene oxide loaded with nano-ZnO, Microbiota community, Secondary bile acid synthesis, Intestinal immune function

Posted Date: April 11th, 2022

DOI: https://doi.org/10.21203/rs.3.rs-1515102/v1

Abstract

Background

To our knowledge, graphene oxide loaded with nano-ZnO (NZnOGO) represent a new nutritional additive for the food and animal husbandry industry. However, the mechanism by which NZnOGO mediates cattle growth and intestinal health are not fully understood. This study was conducted to evaluate the effects of NZnOGO on gut microbiota, bile acid (BA) concentration and intestinal immunity in fattening cattle.

Results

Twenty Simmental × Chinese Yellow Cattle were assigned to 2 dietary groups: control diet (CON) without Zn supplement and CON diet supplemented with NZnOGO. The trial lasted 60 d. The gut microbiota composition and BA concentration in the colon chyme samples were determined by microbiota metagenomics and gas chromatography methods, respectively. Colon mucosa immune factors and gene expression analysis were determined by ELISA and RT-PCR, respectively. The results showed that dietary NZnOGO supplementation significantly increased average daily gain ($P < 0.05$), and significantly decreased feed conversion ratio ($P < 0.05$). The relative abundance of the secondary BA synthesis microbiota genera *Clostridium*, *Ruminococcus*, *Eubacterium*, *Enterococcus*, *Collinsella*, *Fusobacterium*, *Eggerthella*, *Brevibacillus* and *Peptostreptococcus* in the NZnOGO group had significantly higher than the CON group ($P < 0.05$). At the secondary BA synthesis pathway, NZnOGO group had significantly higher 7α-hydroxysteroid dehydrogenase (EC:1.1.1.159) and bile acid-CoA ligase BaiB (EC:6.2.1.7) than the CON group ($P < 0.05$). Dietary NZnOGO supplementation significantly decreased primary BA (taurocholic acid, taurochenodeoxycholic acid and taurodeoxycholate acid) ($P < 0.05$), and significantly increased secondary BA (deoxycholic acid, beta-Muricholic acid, 12-ketolithocholic acid, hyodeoxycholic acid, lithocholic acid, isolithocholic acid, ursodeoxycholic acid and apocholic acid) ($P < 0.05$). The NZnOGO group significantly increased the abundance of gene expression at metabolism and higher defense mechanisms ($P < 0.05$). The expression of Takeda G-protein-coupled receptor 5, protein kinase A, cyclic-AMP response element binding protein, toll-like receptor 4 and interleukin-10 (*IL-10*) genes were increased by dietary NZnOGO supplementation ($P < 0.05$), while the expression of nuclear factor kappa-B (*NF-κB*), tumor necrosis factor-α (*TNF-α*) and *IL-1β* genes were significantly decreased ($P < 0.05$). IL-10 concentration was increased by dietary NZnOGO supplementation ($P < 0.05$), whereas TNF-α and IL-1β contents were significantly decreased ($P < 0.05$).

Conclusions

Taken together, dietary NZnOGO supplementation improved the growth performance and intestinal immune function of the fattening cattle, compared to the diet free of Zn supplement, which was associated with enhancing secondary BA synthesis microbiota growth and promoting secondary BA synthesis.

Introduction

Intestinal microbiota is directly involved in cattle nutritional metabolism, immune activation and resistance to pathogen invasion [1, 2]. There are elegant intercellular communication strategies between intestinal microbiota and host, such as short chain fatty acids, secondary bile acids (BA) and other metabolites as signal molecules to achieve intercellular communication and transmission, so as to regulate intestinal mucosal immune function [3, 4]. The primary BA secreted by the liver can be metabolized by intestinal microbiota to form secondary BA. Secondary BA can bind to Takeda G-protein-coupled receptor 5 (TGR5), up regulate *TGR5* gene's expression, promote the expression of phosphorylation of protein kinase A (*PKA*) and cyclic-AMP response element binding protein (*CREB*) genes, and inhibit nuclear factor κB (NF-κB) signaling pathway, playing a significant anti-inflammatory effect [5, 6]. Consequently, on the basis of understanding the intestinal microbiota-BA-TGR5-PKA signaling pathway to regulate BA metabolism and intestinal mucosal immune function in animals, further research and development of nutritional additives to regulate intestinal microbiota structure, promote secondary BA production and enhance immune function will have an important practical significance for animal production.

Nano zinc oxide (NZnO) promotes growth can act as antibacterial agent, modulates the immunity and reproduction of the cattle [7, 8]. Due to the large surface area, small particle size and high surface free energy, NZnO is easy to agglomerate. In addition, graphene oxide (Go) is a two-dimensional nano material, mostly single-layer sheet structure, with a high specific surface area, rigid structure of sheet layer, sharp edge structure and easy modification, which is outstanding in drug delivery, antibacterial activity, antiviral and other aspects [9–11]. Graphene oxide has the advantages of rich oxygen-containing functional groups such as hydroxyl and carboxyl groups on its surface, relatively simple preparation process, low cost and mass production, which provides a strong support for it as a feed additive carrier. But the rich functional groups on the surface of Go have strong polarity, and it is easy to form agglomeration between the layers, which makes it difficult to dissolve in organic solvents [12]. Previous studies have shown that after the preparation of Go loaded with Nano-ZnO (NZnOGO) by using Go as matrix and loading NZnO on Go surface at low temperature, the properties of NZnOGO are not damaged, and NZnO is uniformly dispersed on GO surface, GO is reduced, and most of the oxygen-containing functional groups on the surface are removed, which effectively solves the agglomeration problem of NZnO and GO [13, 14]. In addition, the conjugated BA secreted by the liver are bio-converted through biological modification (deconjugation, dehydroxylation and epimerization) by intestinal microbiota into secondary BA [15–20]. However, the research of NZnOGO is limited to the materials field. Thus, whether NZnOGO as an animal feed additive can regulate the intestinal microbiota structure, promote secondary BA synthesis through biological modification (deconjugation, dehydroxylation and epimerization), and enhance the immune function need further exploration.

In the intensive feeding of ruminants, in order to meet the high energy needs of short-term fattening cattle, the diet usually contains a high proportion of carbohydrates. This diet mode can cause cattle gastrointestinal metabolic disorder, damage the level of gastrointestinal epithelial barrier function, induce intestinal inflammation [21, 22]. Therefore, we hypothesize that NZnOGO (our own synthetic) alters gut microbiota community to promote secondary BA synthesis, and enhance intestinal immune function by

secondary BA-TGR5-PKA signaling pathway of fattening cattle. Specially, our objectives are to explain the underlying mechanism of NZnOGO for improving animal intestinal health.

Materials And Methods

NZnOGO synthesis

NZnOGO synthesis was performed as previously described [13, 14]. Briefly, pour 100 mL distilled water into the beaker, then added 0.5 g GO, adjusted the pH value to 11 with NaOH, and placed into an electric blast drying oven at 60 °C for 0.5 h of reaction. Then added 25 mL 0.2 mol/L NZnO as zinc source into the water bath pot, mixed, continued stirring for 10 min, reacted at 60 ℃ for 30 min, continuously used 25 mL 4 mol/L NaOH as alkali source for titration, washed the obtained mixture. Finally, put the obtained sample into the oven at 130 ℃ for 2 h, and then dry it at 80 ℃ in the blast drying oven for 24 h.

Animals, experimental design, diets and housing

A total of 20 Simmental × Chinese Yellow Cattle (480 days) with body weight (BW, 411.73 ± 11.68 kg) were selected and randomly assigned into 2 dietary treatments. The control (CON) group was fed with the basic diet (without zinc addition), and the experimental treatment (NZnOGO) group was fed with 80 mg/kg zinc on the basis of the basic diet. The zinc dose were designed as previously described [7, 8]. NZnOGO was prepared by our own synthesis. Basal diet that were formulated to meet or exceed nutrient requirements using the China's beef cattle feeding standard [23]. Ingredients and composition of basic diets are shown in Table 1. The experiment lasted 60 d. All animals were fed in a single pen, which received diet 2 times daily (08. 00~09. 00 and 16. 00~17. 00 h). The experimental cattle were free to drink water.

Growth study

The average daily gain (ADG) of each group was calculated according to the measured body weight. The ADG was calculated as (final weights - initial weight)/60. During the experiment, the actual feed amount per day was recorded. The dry matter content of feed and residual feed was measured every 10 days to calculate the daily average dry matter intake (DMI) within 10 days. The average DMI within 10 days was used to calculate the DMI of the whole experiment period. According to DMI and ADG, the discharge weight ratio was calculated. The feed-to-gain ratio (F:G) was calculated as (total feed intake / total weight gain).

Samples collection

Five cattle were selected for slaughter at each group, and colon chyme samples were collected and frozen in liquid nitrogen at -80 °C for microbiota metagenome and BA composition analysis. Collected intestinal segment of about 5 cm in the middle colon, rinsed the chyme with pre-chilled saline, scraped the intestinal mucosa with a glass slide to the 2 mL cryotube, and stored in liquid nitrogen at -80 °C. Colon mucosa samples were used for the determination of intestinal cytokine and gene expression.

Colon chyme DNA extraction and microbiota metagenomics data analysis

The E.Z.N.A. ® Soil DNA Kit (Omega bio TEK, USA) was used to extract genomic DNA from colon chyme microorganisms. After genomic DNA was extracted, TBS-380 was used to detect DNA concentration, NanoDrop2000 to detect DNA purity and DNA integrity after 1% agarose gel electrophoresis to ensure DNA quality. Covaris M220 was used to break the DNA to about 400 BP. The PE library was constructed by next flex rapid DNA SEQ Kit (Bio scientific, USA), and then amplified by bridge PCR. The metagenome was sequenced by Illumina novaseq/hiseq xten sequencing platform (Illumina, USA). Fastp software was used for quality control of raw data.

The BWA software was used to compare the reads to the DNA sequence of cattle, and the contaminated reads (excluding the host cattle genome: http://asia.ensembl.org/Bos_taurus/Info/Index?db=core) with high alignment similarity was removed. MEGAHIT software was used to splice and assemble the optimized sequence. Contigs ≥ 300 bp were selected as the result of assembly. MetaGene (http://metagene.cb.k.u-tokyo.ac.jp/) was used to predict the ORF of contings in the splicing results [24]. The genes with nucleic acid length greater than or equal to 100 bp were selected and translated into amino acid sequences to obtain the gene prediction results of each sample. SOAPaligner software (http://soap.genomics.org.cn/) compares the high-quality reads of each sample with the non-redundant gene set (the default parameter is 95% identity), and counts the gene abundance information in the corresponding sample. The gene catalogue was translated to putative amino acid sequences, which were aligned against the proteins in NR, evolutionary genealogy of genes: the Kyoto Encyclopedia of Genes and Genomes (KEGG, http://www.genome.jp/kegg/) and Non-supervised Orthologous Groups (EggNOG, http://eggnog. embl.de/) databases with BLASTP (BLAST Version 2.2.28+, http://blast.ncbi.nlm.nih.gov/Blast.cgi) (e-value ≤ 1e-5).

Colon chyme BA content analysis

Accurately weighed 50 mg of colon chyme sample and added 400 μL extract (methanol: water = 4:1), put frozen tissue into grinding instrument grinding for 6 min (-10 °C, 50 Hz), then sonicate it by low temperature ultrasonic instrument for 30 min (5 °C, 40 kHz), -20 °C standing for 30 min, centrifuged at 13,000 × *g* at 4 °C for 15 min to get the supernatant. LC-ESI-MS/MS (UHPLC-Qtrap 6500^{+}) was used for the qualitative determination of BA in samples. Thermo Q exictive mass spectrometer can collect primary and secondary mass spectrometry data under the control of control software (Xcalibur, version: 4.0.27.13, thermo). Waters BEH C18 column (100*2.1 mm, 1.7 μm), column temperature 40 °C. Mobile phase A (0.1% formic acid aqueous solution) and mobile phase B (0.1% formic acid methanol). In the AB Sciex quantitative software OS, the default parameters are used to automatically identify and integrate the ion fragments, and assist the manual inspection.

Standards for taurocholic acid (TCA), taurochenodeoxycholic acid (TCDCA), glycochenodeoxycholic acid (GCDCA), cholic acid (CA), allocholic acid (ACA), taurodeoxycholate acid (TDCA), deoxycholic acid (DCA), taurolithocholic acid (TLCA), beta-Muricholic acid (β-MCA), hyocholic acid (HCA), 12-ketolithocholic acid (12-KLCA), hyodeoxycholic acid (HDCA), murideoxycholic acid (MDCA), omega-murichoclic acid (ω-MCA), lithocholic acid (LCA), isolithocholic acid (isoLCA), glycodeoxycholic acid (GDCA), glycolithocholic acid (GLCA), ursodeoxycholic acid (UDCA), 3β-ursodeoxycholic acid (3β-UDCA), glycoursodeoxycholic acid (GUDCA), apocholic acid (apoCA), dehydrolithocholic acid (DHLCA), 23-

nordeoxycholic acid (NorDCA), 3-dehydrocholic acid (3-DHCA), 12-ketochenodeoxycholicacid (12-KCDCA), 7-ketodeoxycholic acid (7-DHCA), ursocholic acid (UCA) and 3β-Cholic acid (βCA) were purchased from Sigma-Aldrich (Steinheim, Germany). The linear regression standard curve was drawn with the mass spectrum peak area of analyte as ordinate and the concentration of analyte as abscissa. Calculation of sample concentration: the mass spectrum peak area of the sample analyte is substituted into the linear equation to calculate the concentration result.

Intestinal mucosa cytokines and immunoglobulin analysis

Interleukin (IL)-10, IL-1β and tumor necrosis factor-α (TNF-α) in colon mucosa were determined using a cattle ELISA kit (Nanjing Jiancheng Biochemical Reagent Co, Nanjing, China) according to the manufacturer's instructions.

Real-time quantitative PCR

Total RNA was extracted from colon mucosa tissue by Trizol method. RNA integrity, concentration and purity were determined by nucleic acid protein analyzer. Total RNA was reversely transcribed into cDNA by ImProm-II reverse transcriptase (Promega, Fitchburg, WI, USA) according to the kit description. The *Bos taurus beta-actin* (*β-actin*), *TGR5*, *PKA*, *NF-κB* and *TNF-α* genes were designed by primer 5.0 software. The *Bos taurus CREB*, *IL-10* and *IL-1β* genes were designed as previously [25, 26]. The sequence of PCR primers is shown in Table 2. Using the SYBR® Green chimeric fluorescence method (TaKaRa, Dalian, China), the target gene was amplified on the Chromo4 Gradient thermocycler (BIO-RAD, Hercules, CA, USA). Briefly, 0.8 μL each of primers, 10 μL 2×SYBR®Premix Ex TaqTM II (TaKaRa Ex Taq HS, dNTP Mixture, Mg2+, SYBR® Green I) and 2.0 μL cDNA, were included in a 20 μL PCR. The reaction conditions were as follows: pre denaturation at 95 ℃ for 30 s, denaturation at 95 ℃ for 5 s, annealing at 60 ℃ for 30 s, a total of 40 cycles. All target genes were normalized to the endogenous reference gene β-actin by employing an optimized comparative Ct ($2^{-\Delta\Delta Ct}$) value method.

Statistical analyses

The individual animal was considered as the experimental unit for growth performance, one animal per pen was used as the experimental unit for BA content and microbiota metagenome and gene expression analysis. The growth performance, colon chyme BA concentration, mucosa cytokines and gene expression between 2 groups were compared by independent-samples t-test. Correlations between secondary BA synthesis bacterial genera and secondary BA concentration were assessed by Pearson's correlation analysis. Data were shown as means ± SD. Significance was declared at $P<0.05$.

Results

Transmission electron microscope observation

The surface of NZnO is granular and easy to agglomerate (Fig. 1A). Go is lamellar, and the surface of the lamellar is very smooth, but it is easy to form agglomeration between the lamellar (Fig. 1B). The loading of

ZnO onto the GO surface does not change the lamellar structure of GO, and the agglomeration phenomenon of GO is improved. At the same time, it can be seen that ZnO is granular on the GO surface and uniformly distributed on the GO surface (Fig. 1C).

Growth performance

The effects of NZnOGO on growth performance are presented in Table 3. Dietary NZnOGO supplementation significantly increased ADG (P<0.05), and significantly decreased F:G (P<0.05). However, there was no significant difference in initial weight, final weight, and ADFI between the 2 groups (P>0.05).

Microbiota diversity analysis

The relative abundance of bacteria at the phylum level is presented in Fig. 2A. In CON group, the top 6 dominant phyla (>1% at least) were Firmicutes (50.07%), Bacteroidetes (36.99%), Spirochaetes (5.24%), unclassified_d_Bacteria (1.70%), Proteobacteria (1.43%), Tenericutes (1.02%). In NZnOGO group, the top 7 dominant phyla (>1% at least) were Firmicutes (62.08%), Bacteroidetes (26.32%), Spirochaetes (1.14%), unclassified_d_Bacteria (1.61%), Proteobacteria (1.49%), Tenericutes (1.30%), Verrucomicrobia (1.60%).

At the genus level (Fig. 2B), 15 dominant genera were identifified (> 1% at least in both treatment groups). The top 5 dominant genera are *unclassified_o_Clostridiales* (14.21%), *Bacteroides* (8.62%), *unclassified_p_Firmicutes* (6.00%), *Alistipes* (6.92%), *unclassified_o_Bacteroidales* (5.37%) at CON group. The top 5 dominant genera in NZnOGO group are *unclassified_o_Clostridiales* (18.80%), *Bacteroides* (5.71%), *unclassified_p_Firmicutes* (7.58%), *unclassified_f_Ruminococcaceae* (5.52%), *Alistipes* (4.97%).

Principal co-ordinates analysis (PCoA) of the colon chyme microbiota community in fattening cattle fed the NZnOGO vs. CON diet. The results showed that the microbiota clustered separately and axes accounted for 85.07% of the total variation detected for 2 groups, suggesting that certain key bacterial species may characterize microbiota of NZnOGO group (Fig. 2C).

Secondary BA synthesis microbiota analysis

To identify the taxon had the great impact on microbiota community, LEfSe were analyzed differences in the relative abundances of the microbiota community components between the 2 groups (Fig. 3A). Compared with the CON group, including unknown bacteria, 46 microbiota phlotypes were lower and 70 were higher in the NZnOGO group. The cattle fed NZnOGO had increased genera *unclassified_o__Clostridiales*, *unclassified_f__Ruminococcaceae*, *Ruminococcus*, *unclassified_p__Firmicutes*, *Clostridium*, *Akkermansia*, *Evtepia*, *Oscillibacter*, *unclassified_c__Clostridia*, *unclassified_f__Clostridiaceae*, *Romboutsia*, *Pseudoflavonifractor*, *unclassified_p_Candidatus_Saccharibacteria*, *Brevirhabdus*, *Faecalibacterium*, *unclassified_p__Lentisphaerae*, *unclassified_p__Lentisphaerae*, *Paenibacillus*, *unclassified_c__Mollicutes*, *unclassified_f__Eubacteriaceae*, *Flavonifractor*, *unclassified_f__Erysipelotrichaceae*, *unclassified_p__Planctomycetes*, *unclassified_p_Verrucomicrobia* and orders *unclassified_p_Planctomycetes*, *Clostridiales*, *Verrucomicrobiales*, *unclassified_p_Firmicutes*,

Planctomycetales, *o__Bacillales*, *unclassified_c__Clostridia*, *unclassified_p_Candidatus_Saccharibacteria*, *unclassified_c_Mollicutes*, *unclassified_p_Verrucomicrobia*, *unclassified_p_Lentisphaerae* and phyla Firmicutes, Tenericutes, Verrucomicrobia, Candidatus_Saccharibacteria, Lentisphaerae (P<0.05).

To identify the secondary BA synthesis microbiota differs between the 2 groups, LEfSe analysis was performed and differentially abundant taxa were found in both CON and NZnOGO groups. The phyla Firmicutes, Tenericutes, Euryarchaeota and Actinobacteria in the NZnOGO group had significantly higher than the CON group (P<0.05; Fig. 3B). At the genus level (Fig. 3C), the abundance of *Clostridium* (P=0.001031), *Ruminococcus* (P=0.00147), *Eubacterium* (P=0.001917), *Enterococcus* (P=0.01628), *Collinsella* (P=0.03172), *Fusobacterium* (P=0.0133), *Eggerthella* (P=0.004785), *Brevibacillus* (P=0.000149), and *Peptostreptococcus* (P=0.02368) in the NZnOGO group had significantly higher than the CON group (P<0.05).

The pathway analysis of secondary BA synthesis

Based on KEGG pathway database information, ko00121 pathway is a secondary BA synthesis pathway. Welch T test was used to analyze the abundance difference of enzymes in ko00121 pathway between CON group and NZnOGO group (Fig. 4A). NZnOGO group had significantly higher 7α-hydroxysteroid dehydrogenase (EC:1.1.1.159) and bile acid-CoA ligase BaiB (baiB; EC:6.2.1.7) than the CON group (P<0.05; Fig. 4B).

BA concentration analysis

Dietary NZnOGO supplementation significantly decreased primary BA (TCA, TCDCA, and TDCA) concentration (P<0.05), and significantly increased secondary BA (DCA, β-MCA, 12-KLCA, HDCA, LCA, isoLCA, UDCA, and apoCA) concentration (P<0.05; Table 4).

Correlation analysis for secondary BA concentration and the relative abundance of secondary BA synthesis microbiota

A Pearson's correlation matrix was generated to explore the correlation between the secondary BA synthesis bacterial genera and secondary BA concentration that were affected by dietary NZnOGO supplementation (Fig. 5). The concentration of DCA was positively correlated with the genera *Clostridium*, *Ruminococcus*, *Eubacterium*, *Enterococcus*, *Collinsella*, *Peptostreptococcus*, *Eggerthella* and *Brevibacillus* (P<0.05). The concentration of β-MCA was positively correlated with the genera *Clostridium*, *Ruminococcus*, *Eubacterium*, *Enterococcus*, *Collinsella*, *Eggerthella* and *Brevibacillus* (P<0.05). The concentration of 12-KLCA was positively associated with the genera *Clostridium*, *Ruminococcus*, *Eggerthella* and *Brevibacillus*. The concentration of LCA was positively correlated with the genera *Clostridium*, *Ruminococcus*, *Eubacterium*, *Enterococcus*, *Peptostreptococcus*, *Eggerthella* and *Brevibacillus* (P<0.05). The concentration of isoLCA was positively correlated with the genera *Eggerthella* (P<0.05). The concentration of UDCA was positively correlated with the

genera *Eggerthella* and *Brevibacillus* (P<0.05). The concentration of apoCA was positively correlated with the genera *Eggerthella* (P<0.05).

Microbiota function prediction

Compare the non-redundant gene set sequence with the eggNOG database using BLASTP (BLAST Version 2.2.28$^+$, http://blast.ncbi.nlm.nih.gov/Blast.cgi), obtain the clusters of orthogenetic groups of proteins (COG) corresponding to the gene, and then calculate the abundance of the COG using the sum of gene abundances corresponding to the COG. According to the COG abundance of the top 30, Welch T test was used to analyze the category and function between 2 groups. Compared with the CON group, NZnOGO group significantly increased the abundance of genes in category at metabolism, information storage and processing (P<0.05), and significantly decreased the abundance of genes in category at poor characterized, cellular processes and signaling (P<0.05; Fig. 6A).

At function level, NZnOGO group had significantly higher carbohydrate transport and metabolism (G), amino acid transport and metabolism (E), translation, ribosomal structure and biogenesi (J), energy production and conversion (C), transcription (K), defense mechanisms (V), cell cycle control, cell division, chromosome p (D), intracellular trafficking, secretion, and vesicular transport (U), secondary metabolites biosynthesis, transport (Q), cytoskeleton (Z), chromation structure and dynamics (B), extracellular structures (W) and RNA processing and modification (A) than the CON group (P<0.05; Fig. 6B).

Intestinal immune function analysis

Dietary NZnOGO supplementation significantly increased the expression of *TGR5*, *PKA*, *CREB* and *IL-10* genes, while the expression of *NF-κB*, *TNF-α* and *IL-1β* genes were significantly decreased (P<0.05; Fig. 7A). IL-10 concentration was increased by dietary NZnOGO supplementation, whereas TNF-α and IL-1β contents were significantly decreased (P<0.05; Fig. 7B).

Pearson correlation analysis between secondary BA concentration and gene expression was presented in Fig. 7C. *TGR5* gene's expression was positively correlated with the DCA, β-MCA and LCA (P<0.05). *PKA* gene's expression was positively correlated with the β-MCA, 12-KLCA, HDCA, isoLCA, LCA, UDCA and apoCA (P<0.05). *CREB* gene's expression was positively correlated with the DCA, β-MCA, HDCA and UDCA (P<0.05). *NF-κB* gene's expression was negatively correlated with the 12-KLCA, HDCA, isoLCA, LCA and apoCA (P<0.05). *TNF-α* gene's expression was negatively correlated with the DCA, β-MCA, 12-KLCA, LCA and UDCA (P<0.05). *IL-1β* gene's expression was negatively correlated with the 12-KLCA, HDCA, isoLCA and LCA (P<0.05). *IL-10* gene's expression was positively correlated with the DCA, β-MCA, 12-KLCA and apoCA (P<0.05).

Discussion

In the present study, we demonstrated that dietary NZnOGO supplementation increase ADG and decrease F:G of cattle. The results of this study are consistent with the results on supplementation of diverse zinc sources. Calves fed diets supplemented with Zn-Met (equivalent to 80 mg of zinc/d) significantly increased

ADG, and tended to be lower F:G ratio [7]. Based on microstructure observations, NZnO particles are distributed on the surface of GO, which makes NZnOGO have higher specific surface area. Dietary NZnOGO supplementation enhancing growth performance of cattle may be due to increase the proportion of NZnO reaching the gastrointestinal tract, regulate intestinal microbiota structure, enhance the digestion and absorption capacity of gastrointestinal tract for nutrients. However, whether NZnOGO can improve the cattle production performance by regulating intestinal microbiota structure needs further study.

The gut microbiota structure is highly related to cattle health and metabolic capacity [27, 28]. The results of this test indicated that there was no difference in the microbiota structure of cattle. Previous studies found that the phyla Firmicutes and Bacteroidetes were the dominated bacterial communities in cattle [27, 28]. Firmicutes mediates the BA biological modification by producing hydroxyl steroid dehydrogenase [29]. In this study, we found that dietary NZnOGO supplementation increased phyla Firmicutes, which suggests that NZnOGO may be involved in the process of secondary BA synthesis. It has been reported that the phyla Actinobacteria, Euryarchaeota and Tenericutes participate in the secondary BA synthesis by producing hydroxyl steroid dehydrogenase, which oxidizes the hydroxyl groups at positions 3, 7 or 12 of the ring chain [29, 30]. Meanwhile, we also found that dietary NZnOGO supplementation increased phyla Actinobacteria, Euryarchaeota and Tenericutes. All these data indicated that NZnOGO can mediate the BA biological modification of cattle.

Primary BA are modified into functional secondary BA by intestinal microbiota through biological processes such as deconjugation, dehydroxylation and epimerization [15-20]. The current experiments show that NZnOGO decreased primary BA (TCA, TCDCA, and TDCA) concentrations, indicating that NZnOGO may enhance the conversion of primary BA to secondary BA. At the processes of BA deconjugation, the intestinal microbiota genera bile salt hydrolase (BSH) secreted by *Brevibacillus* and *Clostridium* deconjugates at C24 amide bonds to convert conjugated BA into free BA [15, 17, 20]. Then, dehydroxylation of deconjugated BA occurs under the action of 7α-dehydroxylase by *Clostridium*, *Eubacterium*, *Eggerthella* and *Ruminococcus* [19, 31]. Our results indicate that NZnOGO increased the relative abundance of *Clostridium*, *Eubacterium*, *Eggerthella* and *Ruminococcus*, demonstrating that NZnOGO may participate in the secondary BA synthesis by BA deconjugation and dehydroxylation processes. It has been reported that β-MCA was converted to HDCA by (3α-, 7α-, 12α)-dehydroxylase, CA was converted to DCA by 7α-dehydroxylation, CDCA was converted to LCA or isoLCA by 7α-dehydroxylation, and CCDCA was converted to HDCA and 12-KLCA by 7α-dehydroxylation [31-35]. The baiB (EC:6.2.1.7) enzyme participates in an anaerobic BA 7α-dehydroxylatio pathway [36, 37]. In this study, we also found that dietary NZnOGO supplementation increased secondary BA (DCA, β-MCA, HDCA, LCA, isoLCA, and 12-KLCA), which may also explain the increased relative abundance of secondary BA-producing *Clostridium*, *Eggerthella*, *Eubacterium*, and *Ruminococcus* by raising baiB (EC:6.2.1.7) abundance in the intestine. The Pearson's correlation confirmed that DCA, β-MCA and LCA were positively correlated with the genera *Clostridium*, *Ruminococcus*, *Eggerthella* and *Eubacterium*, respectively. 12-KLCA was positively correlated with the genera *Clostridium*, *Ruminococcus* and *Eggerthella*. Our data show that the relative abundance of secondary BA microbiota (*Clostridium*, *Ruminococcus*, *Eggerthella* and *Eubacterium*) are

increased in NZnOGO group, which could promote secondary BA (DCA, β-MCA, HDCA, LCA, isoLCA, and 12-KLCA) production by raising baiB (EC:6.2.1.7) abundance at the processes of BA deconjugation and dehydroxylation.

At the process of BA epimerization processes, the intestinal microbiota genera *Clostridium*, *Ruminococcus*, *Eubacterium*, *Escherichia*, *Peptostreptococcus*, *Fusobacterium*, *Enterococcus*, and *Collinsella* use the hydroxylsteroid dehydrogenases (HSDHs) family to perform epimerization or oxidation [15, 19]. In our study, we found that NZnOGO supplementation increased the relative abundance of secondary BA-producing *Clostridium*, *Ruminococcus*, *Eubacterium*, *Enterococcus*, *Peptostreptococcus*, *Enterococcus* and *Collinsella*. These changes suggest that NZnOGO may be involved in the secondary BA synthesis by BA epimerization process. At the secondary BA synthesis pathway, previous studies demonstrated 7α-HSDHs are key biocatalysts for the biotransformation of UDCA from chenodeoxycholic acid CDCA [38]. CDCA generates UDCA and DCA under 7α/β-epimerization [39]. 12-KLCA is an important intermediate for the synthesis of UDCA [40]. UDCA is converted to LCA by 7β-dehydroxylase, isoLCA is formed of LCA. β-MCA converted to ω-MCA by 6β-epimerization, then produces HDCA by 7β-dehydroxylation, or forms HCA by 7β-epimerization [15, 39, 41, 42]. In this experiment, we also found that dietary NZnOGO supplementation increased secondary BA (UDCA, DCA, LCA, isoLCA, β-MCA, and HDCA), which may also explain the increased relative abundance of secondary BA-producing *Clostridium*, *Ruminococcus*, *Eubacterium*, *Enterococcus*, *Peptostreptococcus* and *Collinsella* by raising 7α-HSDHs (EC:1.1.1.159) abundance in the intestine. Next, to investigate the connection between BA epimerization bacteria and secondary BA (UDCA, DCA, LCA, isoLCA, β-MCA, and HDCA), we compared the taxa revealed by LEfSe analysis to the secondary BA. Current results showed that β-MCA was positively correlated with the genera *Clostridium*, *Ruminococcus*, *Eubacterium*, and *Collinsella*. LCA was positively correlated with the genera *Clostridium*, *Ruminococcus*, *Eubacterium*, and *Peptostreptococcus*. Taken altogether, these data indicate that dietary NZnOGO supplementation increases secondary BA (UDCA, DCA, LCA, isoLCA, β-MCA, and HDCA) through increasing the relative abundance of secondary BA microbiota genera *Clostridium*, *Ruminococcus*, *Eubacterium*, *Escherichia*, *Peptostreptococcus* and *Collinsella* by raising 7α-HSDHs (EC:1.1.1.159) abundance at the BA epimerization processes.

Our data show that NZnOGO increases the abundance of genes at metabolism and higher defense mechanisms at category and function level of COG Orthology analysis, suggesting that NZnOGO may enhance intestinal mucosal immunity of cattle. Moreover, after biological modification of intestinal microbiota, secondary BA can interact with intestinal mucosal immunity, strengthen its barrier function, and prevent or treat mucosal inflammation and other intestinal diseases [43-45]. The UDCA reduced the levels of inflammatory factors (TNF-α, IL-6) and inhibited intestinal villus injury, indicating that UDCA has anti-inflammatory activity and cell protective effects [43]. Supplementation of LCA by enema could prevent apoptosis of colonic epithelial cells and enhance mucosal immune barrier function in mice [43]. As a metabolic derivative of LCA flora, isoLCA affects host intestinal mucosal immunity by regulating the differentiation of Th17 cells and Treg cells in mice [45]. IsoDCA produced by biological modification of DCA can regulate intestinal immune function [46]. In this experiment, our findings show that dietary NZnOGO supplementation increases secondary BA (DCA, β-MCA, 12-KLCA, HDCA, LCA, isoLCA,

UDCA, and apoCA) contents, which may also explain NZnOGO increases the abundance of genes at metabolism and higher defense mechanisms at category and function level of COG Orthology analysis. Taken altogether, it is implied that NZnOGO enhance intestinal mucosal immunity of cattle.

TGR5 is a member of G protein coupled receptor family, which has been shown to play a role in inflammation [5, 6]. Previous studies also show that DCA, LCA and UDCA can directly act on intestinal epithelial TGR5 receptor to down-regulate the expression of inflammatory factors, and enhance intestinal immune function [31, 45, 47]. Secondary BA up-regulated the *TGR5* gene's expression, activated the receptors on the membrane, phosphorylated PKA, promoting the expression of *CREB* gene, and down-regulating the expression of *NF-κB* gene, reducing the expression and secretion of pro-inflammatory cytokines such as TNF-α and IL-1β, and increasing the expression and secretion of anti-inflammatory cytokines such as IL-10 [48, 49]. To further evaluate the intestinal immune function of cattle, we determined the BA-TGR5-CREB regulation NF-κB signaling pathway in the intestinal mucosa. In our study, we found that dietary NZnOGO supplementation up-regulated the expression of *TGR5*, *PKA*, *SREBP-1* and *IL-10* genes, down-regulated the expression of *NF-κB*, *TNF-α* and *IL-1β* genes, and reduced TNF-α and IL-1β concentrations. The Pearson's correlation also confirmed that DCA and LCA were positively correlated with the *TGR5* gene's expression. Taking all the evidence together, it indicates that NZnOGO enhance intestinal mucosal immunity of cattle by regulating intestinal microbiota-BA-TGR5 signaling pathway.

Conclusions

In conclusion, NZnOGO promotes the growth performance and enhances intestinal immune function of the fattening cattle, compared to the diet free of Zn supplement. These functions of NZnOGO are associated, partly, with benefiting secondary BA synthesis microbiota growth and promoting secondary BA synthesis by microbiota biological modification (deconjugation, dehydroxylation and epimerization), modulating secondary BA-TGR5-PKA signaling pathway, and changes of the immune status (Fig. 8).

Abbreviations

BW
body weight
ADFI
average daily feed intake
ADG
average daily gain
F
G:feed-to-gain ratio
CON
control
NZnOGO
graphene oxide loaded with Nano-ZnO

BA
bile acid
TCA
taurocholic acid
TCDCA
taurochenodeoxycholic acid
GCDCA
glycochenodeoxycholic acid
CA
cholic acid
ACA
allocholic acid
TDCA
taurodeoxycholate acid
DCA
deoxycholic acid
TLCA
taurolithocholic acid
β-MCA
beta-Muricholic acid
HCA
hyocholic acid
12-KLCA
12-ketolithocholic acid
HDCA
hyodeoxycholic acid
MDCA
murideoxycholic acid
ω-MCA
omega-murichoclic acid
LCA
lithocholic acid
isoLCA
isolithocholic acid
GDCA
glycodeoxycholic acid
GLCA
glycolithocholic acid
UDCA
ursodeoxycholic acid
3β-UDCA

3β-ursodeoxycholic acid
GUDCA
glycoursodeoxycholic acid
apoCA
apocholic acid
DHLCA
dehydrolithocholic acid
NorDCA
23-nordeoxycholic acid
3-DHCA
3-dehydrocholic acid
12-KCDCA
12-ketochenodeoxycholicacid
UCA
ursocholic acid
7-DHCA
7-ketodeoxycholic acid
βCA
3β-cholic acid
TGR5
Takeda G-protein-coupled receptor 5
PKA
protein kinase A
CREB
cyclic-AMP response element binding protein
IL-10
interleukin-10
NF-κB
nuclear factor kappa-B
TNF-α
tumor necrosis factor-α
IL-1β
interleukin-1 β.

Declarations

Acknowledgements

Not applicable.

Authors' contributions

H. Zhang. and L. Li. designed research. W. Guan., Q. Xing. and C. Huang. conducted research. H. Zhang. and D. Guo. analyzed data and wrote the paper. C. Xiong., Bao. Li., K. Chen. and C. Peng. reviewed the paper. The authors read and approved the final manuscript.

Funding

This study was financially supported by National Natural Science Foundation of China (grant number 32060773 and 32160804), Jiangxi Provincial Department of Education Science and Technology Research Project (grant number GJJ201621 and GJJ190848), and Natural Science Foundation of Jiangxi Province (grant number 20202BABL205010).

Availability of data and materials

The data produced or analyzed during the current study are available from the corresponding author by reasonable request.

Ethics approval and consent to participate

All animals were conducted under the Chinese guidelines for animal welfare. The experimental protocol and procedures were in accordance with the Yichun University Institutional Animal Care and Use Committee.

Consent for publication

Not applicable.

Competing interests

The authors declare that they have no conflict of interest.

Author details

[a] College of Life Science and Resources and Environment, Yichun University, Yi Chun 336000, China

[b] Engineering Technology Research Center of Jiangxi Universities and Colleges for Selenium Agriculture, Yichun University, Yi Chun 336000, China

References

1. Kirkpatrick BW. Lett BM. Heritability of susceptibility to infection by Mycobacterium avium ssp. paratuberculosis in Holstein cattle. J Dairy Sci. 2018;101(12):11165–9.
2. O'Hara E. Neves ALA, Song Y. Guan LL. The role of the gut microbiome in cattle production and health: driver or passenger? Annu Rev Anim Biosci. 2020;8:199–220.
3. Rahimi S, Kathariou S, Fletcher O, Grimes JL. The effectiveness of a dietary direct-fed microbial and mannan oligosaccharide on ultrastructural changes of intestinal mucosa of turkey poults infected with *Salmonella* and *Campylobacter*. Poult Sci. 2020;99:1135–49.

4. Song X, Sun X, Oh SF, Wu M, Zhang Y, Zheng W, et al. Microbial bile acid metabolites modulate gut RORγ^{+} regulatory T cell homeostasis. Nature. 2020;577:410–5.
5. Carino A, Marchiano S, Biagioli M, Bucci M, Vellecco V, Brancaleone V, et al. Agonism for the bile acid receptor GPBAR1 reverses liver and vascular damage in a mouse model of steatohepatitis. Faseb J. 2019;33:2809–22.
6. Andrade JM, Faustino C, Garcia C, Ladeiras D, Reis CP, Rijo P. *Rosmarinus officinalis* L.: an update review of its phytochemistry and biological activity. J Drug Deliv Ther. 2019;9:323–30.
7. Chang MN, Wei JY, Hao LY, Ma FT, Li HY, Zhao SG, Sun P. Effects of different types of zinc supplement on the growth, incidence of diarrhea, immune function, and rectal microbiota of newborn dairy calves. J Dairy Sci. 2020;103(7):6100–13.
8. Kumar S, Kumar V, Kumar M, Vaswani S, Kushwaha R, Kumar A, et al. Comparing efficacy of nano zinc on performance, nutrient utilization, immune and antioxidant status in hariana cattle. P Natl A Sci India B. 2021;91(3):707–13.
9. Dasari Shareena TP, McShan D, Dasmahapatra AK, Tchounwou PB. A review on graphene-based nanomaterials in biomedical applications and risks in environment and health. Nano-Micro Lett. 2018;10:164–97.
10. Jafari Z, Baharfar R, Rad AS, Asghari S. Potential of graphene oxide as a drug delivery system for Sumatriptan: a detailed density functional theory study. J Biomol Struct Dyn. 2021;39:1611–20.
11. Jihad MA, Noori FTM, Jabir MS, Albukhaty S, AlMalki FA, Alyamani AA. Polyethylene glycol functionalized graphene oxide nanoparticles loaded with nigella sativa extract: a smart antibacterial therapeutic drug delivery system. Molecules. 2021;26:3067–83.
12. Lu H, Zhang S, Guo L, Li W. Applications of graphene-based composite hydrogels: a review. RSC Adv. 2017;7:51008–20.
13. Li B, Liu T, Wang Y, Wang Z. ZnO/graphene-oxide nanocomposite with remarkably enhanced visible-light-driven photocatalytic performance. J Colloid Interf Sci. 2012;377:114–21.
14. Dhanalakshmi N, Priya T, Thennarasu S, Sivanesan S, Thinakaran N. Synthesis and electrochemical properties of environmental free L-glutathione grafted graphene oxide/ZnO nanocomposite for highly selective piroxicam sensing. J Pharm Anal. 2021;11:48–56.
15. Ridlon JM, Harris SC, Bhowmik S, Kang DJ, Hylemon PB. Consequences of bile salt biotransformations by intestinal bacteria. Gut Microbes. 2016;7:22–39.
16. Jia W, Xie G, Jia W. Bile acid-microbiota crosstalk in gastrointestinal inflammation and carcinogenesis. Nat Rev Gastro Hepat. 2018;15:111–28.
17. Sheng L, Jena PK, Liu HX, Hu Y, Nagar N, Bronner DN, et al. Obesity treatment by epigallocatechin-3-gallate-regulated bile acid signaling and its enriched *Akkermansia muciniphila*. Faseb J. 2018;32:6371–84.
18. Pathak P, Xie C, Nichols RG, Ferrell JM, Boehme S, Krausz KW, et al. Intestine farnesoid X receptor agonist and the gut microbiota activate G-protein bile acid receptor-1 signaling to improve metabolism. Hepatology. 2018;68:1574–88.

19. Brown JM, Hazen SL. Microbial modulation of cardiovascular disease. Nat Rev Microbiol. 2018;16:171–81.
20. Mullish BH, Mcdonald JAK, Pechlivanis A, Allegretti JR, Kao D, Barker GF, et al. Microbial bile salt hydrolases mediate the efficacy of faecal microbiota transplant in the treatment of recurrent *Clostridioides difficile* infection. Gut. 2019;68:1791–800.
21. Tian K, Liu J, Sun Y, Wu Y, Chen J, Zhan R, et al. Effects of dietary supplementation of inulin on rumen fermentation and bacterial microbiota, inflammatory response and growth performance in finishing beef steers fed high or low-concentrate diet. Anim Feed Sci Tech. 2019;258:114299–311.
22. Liu J, Tian K, Sun Y, Wu Y, Chen J, Zhang R, et al. Effects of the acid–base treatment of corn on rumen fermentation and microbiota, inflammatory response and growth performance in beef cattle fed high-concentrate diet. Animal. 2020;1–9.
23. MAPRC. Feeding standard of beef cattle (NY/T 815–2004. Beijing: China Agricultural Publishing House; 2004.
24. Noguchi H, Park J, Takagi T. MetaGene: prokaryotic gene finding from environmental genome shotgun sequences. Nucleic Acids Res. 2006;34:5623–30.
25. Wei D, Ma X, Zhang S, Hong J, Gui L, Mei C, et al. Characterization of the promoter region of the bovine SIX1 gene: roles of MyoD, PAX7, CREB and MyoG. Sci Rep-Uk. 2017;7:12599–600.
26. Lahouassa H, Moussay E, Rainard P, Riollet C. Differential cytokine and chemokine responses of bovine mammary epithelial cells to *Staphylococcus aureus* and *Escherichia coli*. Cytokine. 2007;38:12–21.
27. Mao S, Zhang M, Liu J, Zhu W. Characterising the bacterial microbiota across the gastrointestinal tracts of dairy cattle: membership and potential function. Sci Rep. 2015;5:16116–30.
28. Clemmons BA, Voy BH, Myer PR. Altering the gut microbiome of cattle: considerations of host-microbiome interactions for persistent microbiome manipulation. Microb Ecol. 2019;77:523–36.
29. Kisiela M, Skarka A, Ebert B, Maser E. Hydroxysteroid dehydrogenases (HSDs) in bacteria-a bioinformatic perspective. J Steroid Biochem. 2012;129:31–46.
30. Islam KBMS, Fukiya S, Hagio M, Fujii N, Ishizuka S, Ooka T. Bile acid is a host factor that regulates the composition of the cecal microbiota in rats. Gastroenterology. 2011;141:1773–81.
31. Fiorucci S, Biagioli M, Zampella A, Distrutti E. Bile acids activated receptors regulate innate immunity. Front Immunol. 2018;9:1853–1840.
32. Thomas C, Pellicciari R, Pruzanski M, Auwerx J, Schoonjans K. Targeting bile-acid signalling for metabolic diseases. Nat Rev Drug Discov. 2008;7:678–93.
33. Degirolamo C, Rainaldi S, Bovenga F, Murzilli S, Moschetta A. Microbiota modification with probiotics induces hepatic bile acid synthesis via downregulation of the Fxr-Fgf15 axis in mice. Cell Rep. 2014;7:12–8.
34. Devlin AS, Fischbach MA. A biosynthetic pathway for a prominent class of microbiota-derived bile acids. Nat Chem Biol. 2015;11:685–90.

35. Winston JA, Theriot CM. Diversification of host bile acids by members of the gut microbiota. Gut Microbes. 2020;11:158–71.
36. Mihalik SJ, Steinberg SJ, Pei Z, Park J, Kim DG, Heinzer AK, et al. Participation of 2 members of the very long-chain acyl-CoA synthetase family in bile acid synthesis and recycling. J Biol Chem. 2002;277:24771–80.
37. Ridlon JM, Kang DJ, Hylemon PB. Isolation and characterization of a bile acid inducible 7α-dehydroxylating operon in *Clostridium hylemonae* TN271. Anaerobe. 2009;16:137–46.
38. Zhang X, Fan D, Hua X, Zhang T. Large-scale production of ursodeoxycholic acid from chenodeoxycholic acid by engineering 7α- and 7β-hydroxysteroid dehydrogenase. Bioproc Biosyst Eng. 2019;42:1537–45.
39. Zheng MM, Wang RF, Li CX, Xu JH. Two-step enzymatic synthesis of ursodeoxycholic acid with a new 7β-hydroxysteroid dehydrogenase from Ruminococcus torques. Process Biochem. 2015;50:598–604.
40. Huang B, Zhao Q, Zhou JH, Xu G. Enhanced activity and substrate tolerance of 7α-hydroxysteroid dehydrogenase by directed evolution for 7-ketolithocholic acid production. Appl Microbiol Biotechnol. 2019;103(6):2665–74.
41. Chiang JYL. Bile acids: regulation of synthesis: thematic review series: bile acids. J Lipid Res. 2009;50:1955–66.
42. Gérard P. Metabolism of cholesterol and bile acids by the gut microbiota. Pathogens. 2014;3:14–24.
43. Kozoni V, Tsioulias G, Shiff S, Rigas B. The effect of lithocholic acid on proliferation and apoptosis during the early stages of colon carcinogenesis: differential effect on apoptosis in the presence of a colon carcinogen. Carcinogenesis. 2000;21:999–1005.
44. Kim S, Chun H, Choi H, Kim E, Keum B, Seo Y, et al. Ursodeoxycholic acid attenuates 5-fluorouracil-induced mucositis in a rat model. Oncol Lett. 2018;16:2585–90.
45. Hang S, Paik D, Yao L, Kim E, Jamma T, Lu J, et al. Bile acid metabolites control TH17 and Treg cell differentiation. Nature. 2019;576:143–8.
46. Josefowicz SZ, Niec RE, Kim HY, Treuting P, Chinen T, Zheng Y, et al. Extrathymically generated regulatory T cells control mucosal TH2 inflammation. Nature. 2012;482:395–9.
47. Wang J, Zhang J, Lin X, Wang Y, Wu X, Yang F, et al. DCA-TGR5 signaling activation alleviates inflammatory response and improves cardiac function in myocardial infarction. J Mol Cell Cardiol. 2021;151:3–14.
48. Wei K, Dai J, Wang Z, Pei Y, Chen Y, Ding Y, et al. Oxymatrine suppresses IL-1β-induced degradation of the nucleus pulposus cell and extracellular matrix through the TLR4/NF-κB signaling pathway. Exp Biol Med. 2020;245:532–41.
49. Zhou Y, Ren Z, Zhang S, Wang H, Wu S, Bao W. Analysis of intestinal mucosa integrity and GLP-2 gene functions upon porcine epidemic diarrhea virus infection in pigs. Animal. 2021;11:644–59.

Tables

Table 1

Report the feed ingredients and chemical composition on a DM basis.

Ingredient composition	Content
Corn grain, %	31.96
Wheat bran, %	28.12
Rapeseed meal, %	5.17
Distillers' grains, %	10.00
Rice straw, %	20.00
Limestone, %	1.15
Salt, %	0.60
Sodium bicarbonate, %	2.00
Premix[1], %	1.00
Nutrition composition[2]	
Net energy, MJ/Kg	6.91
Crude protein, %	12.44
Neutral detergent fiber, %	32.07
Acid detergent fiber, %	21.13
Calcium, %	0.71
Phosphorus, %	0.72
Zn, mg/kg	29.22

[1]Vitamin premix provided the following per kilogram diet: 1,250 IU of vitamin A, 0.1 mg of Co, 9 mg of Cu, 0.6 mg of I, 54 mg of Mn, 0.2 mg of Se, and 33 mg of monensin.

[2]Net energy, Calcium and Phosphorus were calculated values according to Feeding Standard of Beef Cattle (NY/T 815-2004), while others were measured values.

Table 2

Specific primers used for real-time quantitative PCR.

Gene	Primer	Product length, bp	Annealing temperature (°C)	Accession
β-actin	F 5’-CAGCAAGCAGGAGTACGATG-3’ R 5’-AGCCATGCCAATCTCATCTC-3’	138	65	NM_173979.3
TGR5	F 5’-AGCATCCATCCATCTTGG-3’ R 5’-GCTTTATTCAGTCAGAGTGGG-3’	142	66	Gene ID: 317756
PKA	F 5’-GACCGAAGCCTGAGTGACAG-3’ R 5’-CAGCTATGTACATCCTCGCG-3’	148	66	Gene ID: 282322
CREB	F 5’-GAGCCATTGATTTGTGCAAAGATG-3’ F 5’-GCGAGTGGTGAGAAGCGAAGTG-3’	165	60	Wei et al. (2017)
NF-κB	F 5’-GGGTTAGCAAGGGATTGAAG-3’ R 5’-CCAGGAAGACATCACCCAAG-3’	118	65	NM_001080242
TNF-α	F 5’-TCTTCTCAAGCCTCAAGTAACAAGC-3’ R 5’-CCATGAGGGCATTGGCATAC-3’	104	69	NM_173966.3
IL-1β	F 5’-CTCTCACAGGAAATGAACCGAG-3’ R 5’-CGCTGCAGGGTGGGCGTATCACC-3’	152	67	Lahouassa et al. (2007)
IL-10	F 5’-GTGATGCCACAGGCTGAGAA-3’ R 5’-TGCTCTTGTTTTCGCAGGGCAG-3’	131	69	Lahouassa et al. (2007)

TGR5 = Takeda G-protein-coupled receptor 5; PKA = protein kinase A; CREB = cyclic-AMP response element binding protein; IL-10 = interleukin-10; NF-κB = nuclear factor kappa-B; TNF-α = tumor necrosis factor-α; IL-

1β = interleukin-1 β.

Table 3

Effects of dietary NZnOGO supplementation on growth performance of fattening cattle[1].

Item	CON group	NZnOGO group
Initial BW, kg	409.88±10.24	413.58±12.69
Final BW, kg	466.76±13.33	484.34±9.29
ADG, kg/day	0.95±0.07[b]	1.18±0.15[a]
ADFI, kg	8.17±0.30	8.10±0.27
F:G	8.66±0.68[a]	6.97±0.80[b]

CON = control; Nano zinc oxide = NZnO; NZnOGO = graphene oxide loaded with Nano-ZnO; BW = body weight; ADFI = average daily feed intake; ADG = average daily gain; F:G = feed-to-gain ratio .

[1]Data are expressed as means ± SD, $n = 10$.

[a, b] Within a row, values with different superscripts indicate a significant difference ($P<0.05$).

Table 4

Effects of dietary NZnO-GO supplementation on colon chyme BA content[1].

Item	CON group	NZnOGO group
Primary BA, ng/ml		
TCA	10.284±2.115[a]	6.199±0.484[b]
TCDCA	0.966±0.155[a]	0.560±0.045[b]
GCDCA	1.641±0.307	0.974±0.667
CA	3.730±1.859	2.795±0.936
ACA	0.217±0.109	0.163±0.054
TDCA	3.339±0.441[a]	1.890±0.449[b]
Secondary BA, ng/ml		
DCA	51.181±3.539[b]	62.579±6.740[a]
TLCA	0.140± 0.026	0.116±0.026
β-MCA	0.532±0.081[b]	0.804±0.094[a]
HCA	0.082±0.016	0.088±0.036
12-KLCA	7.887±0.798[b]	10.262±0.220[a]
HDCA	1.961± 0.372[b]	2.707±0.244[a]
MDCA	0.082±0.008	0.087±0.022
ω-MCA	0.022±0.011	0.018±0.010
LCA	12.746±0.247[b]	14.699±0.878[a]
isoLCA	3.115±0.299[b]	3.989±0.419[a]
GDCA	5.027±1.105	5.974±0.883
GLCA	0.031±0.009	0.036±0.003
UDCA	1.496±0.299[b]	2.146±0.117[a]
3β-UDCA	0.278±0.035	0.274±0.072
GUDCA	0.012±0.004	0.015±0.006
apoCA	0.632±0.071[b]	0.817±0.061[a]
DHLCA	2.880±0.543	3.420±0.646
NorDCA	0.180±0.059	0.218±0.013
3-DHCA	0.127±0.021	0.109±0.021
12-KCDCA	0.258±0.094	0.206±0.036
UCA	0.054±0.009	0.072±0.016
7-DHCA	1.398±0.371	1.469±0.264
βCA	0.027±0.008	0.027±0.007

CON = control; NZnOGO = graphene oxide loaded with Nano-ZnO; BA = bile acid; TCA = taurocholic acid; TCDCA = taurochenodeoxycholic acid; GCDCA = glycochenodeoxycholic acid; CA = cholic acid; ACA = allocholic acid; TDCA = taurodeoxycholate acid; DCA = deoxycholic acid; TLCA = taurolithocholic acid; β-MCA = beta-Muricholic acid; HCA = hyocholic acid; 12-KLCA = 12-ketolithocholic acid; HDCA = hyodeoxycholic acid; MDCA = murideoxycholic acid; ω-MCA = omega-murichoclic acid; LCA = lithocholic acid; isoLCA = isolithocholic acid; GDCA = glycodeoxycholic acid; GLCA = glycolithocholic acid; UDCA = ursodeoxycholic acid; 3β-UDCA = 3β-ursodeoxycholic acid; GUDCA = glycoursodeoxycholic acid; apoCA = apocholic acid; DHLCA = dehydrolithocholic acid; NorDCA = 23-nordeoxycholic acid; 3-DHCA = 3-dehydrocholic acid; 12-KCDCA = 12-ketochenodeoxycholicacid; UCA = ursocholic acid; 7-DHCA = 7-ketodeoxycholic acid; βCA = 3β-cholic acid.

[1]Data are expressed as means ± SD, n = 5.

[a, b] Within a row, values with different superscripts indicate a significant difference ($P<0.05$).

Figures

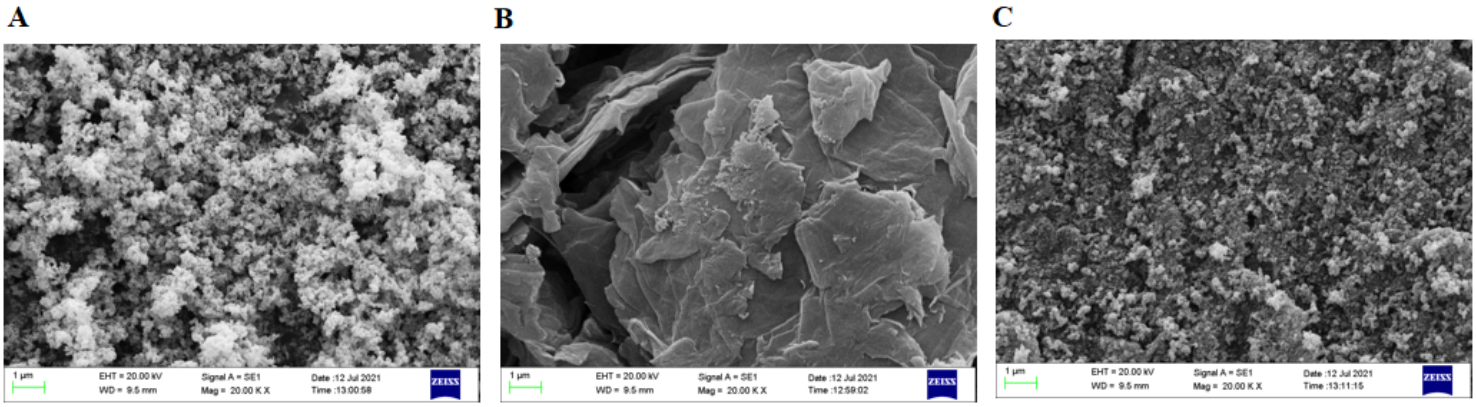

Figure 1

Morphologies of NZnO, Go and NZnOGO. (A) NZnO morphologies, (B) Go morphologies, (C) NZnOGO morphologies. NZnO = nano-ZnO; Go = graphene oxide; NZnOGO = graphene oxide loaded with NZnO.

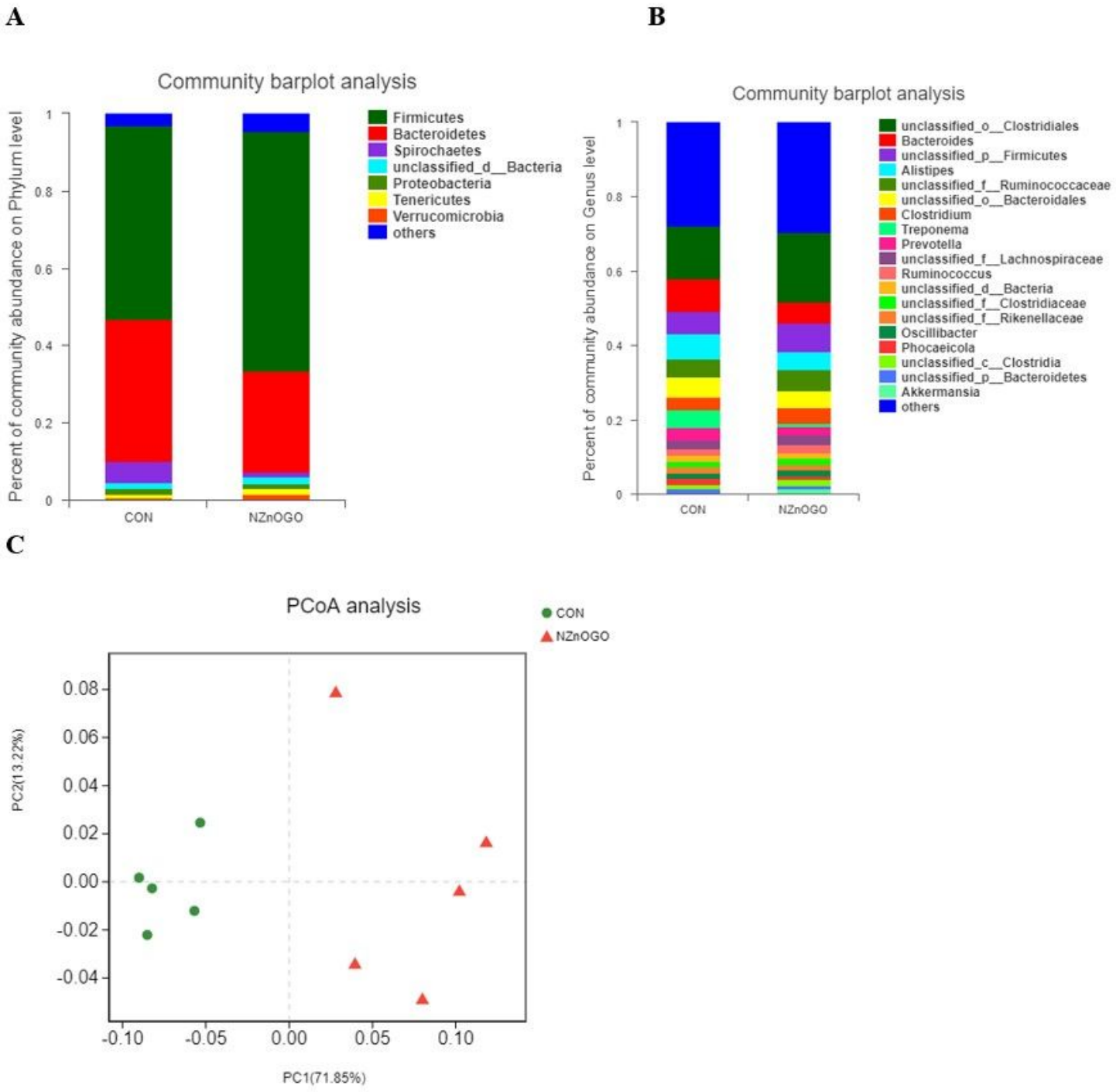

Figure 2

Effect of NZnOGO on colon chyme microbiota diversity. (A) phylum level, (B) genus level, (C) principal co-ordinates analysis (PCoA). Cattle were regarded as the experimental units, *n* = 5 for each group. CON = control; NZnOGO = graphene oxide loaded with nano-ZnO.

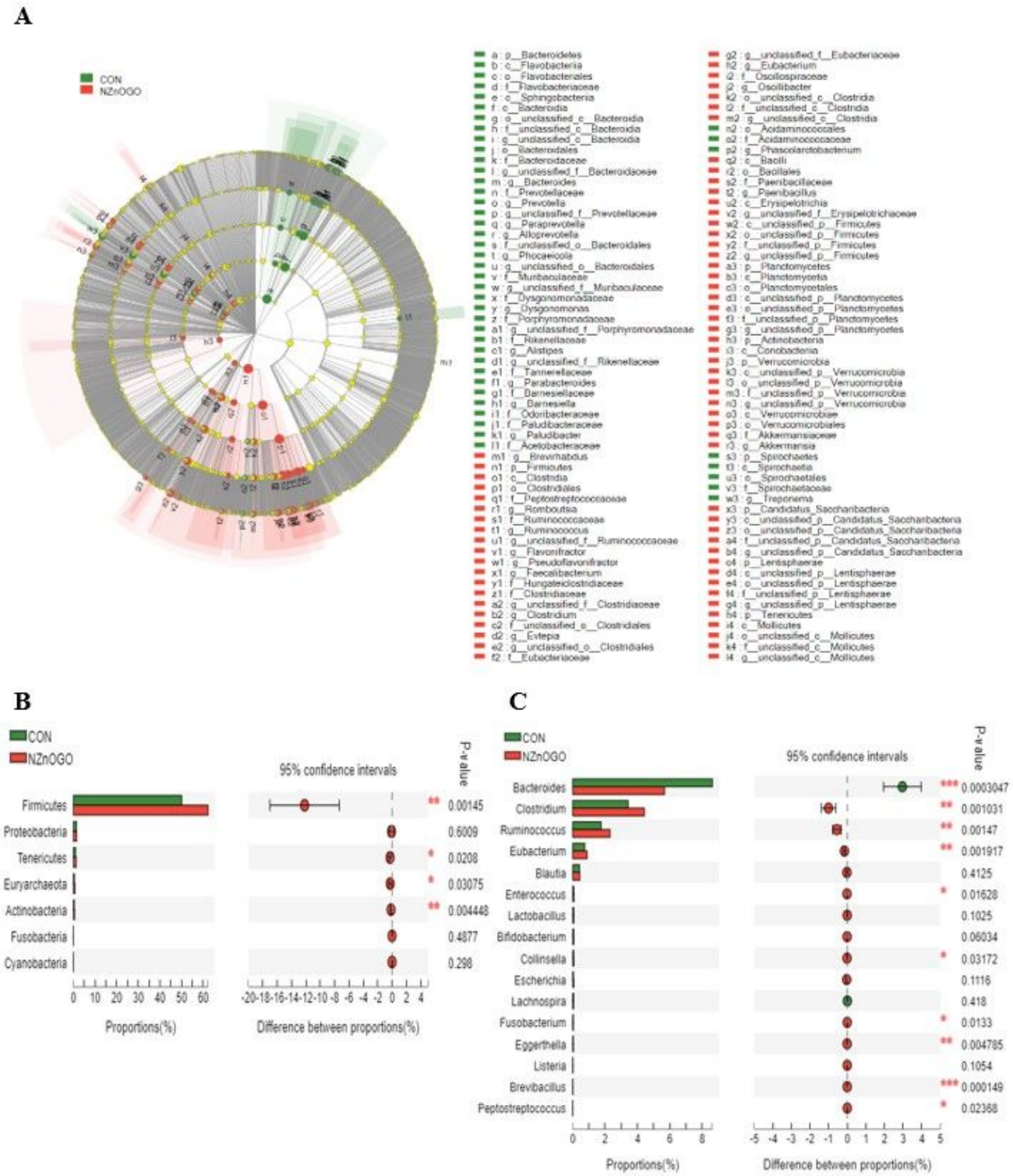

Figure 3

Differential colonic chyme microbiota communities change between 2 groups. (A) Differ colon chyme bacterial community, (B) The Welch's t-test on secondary BA synthesis microbiota at phylum, (C) The Welch's t-test on secondary BA synthesis microbiota at genus. LDA ≥ 2.5 and $P \leq 0.05$ are shown. CON = control; NZnOGO = graphene oxide loaded with nano-ZnO; BA = bile acid; LDA = linear discriminant analysis; p_ = phylum; c_ = class; o_ = order; f_ = family; g_ = genus. Cattle were regarded as the experimental units, n = 5 for each grou

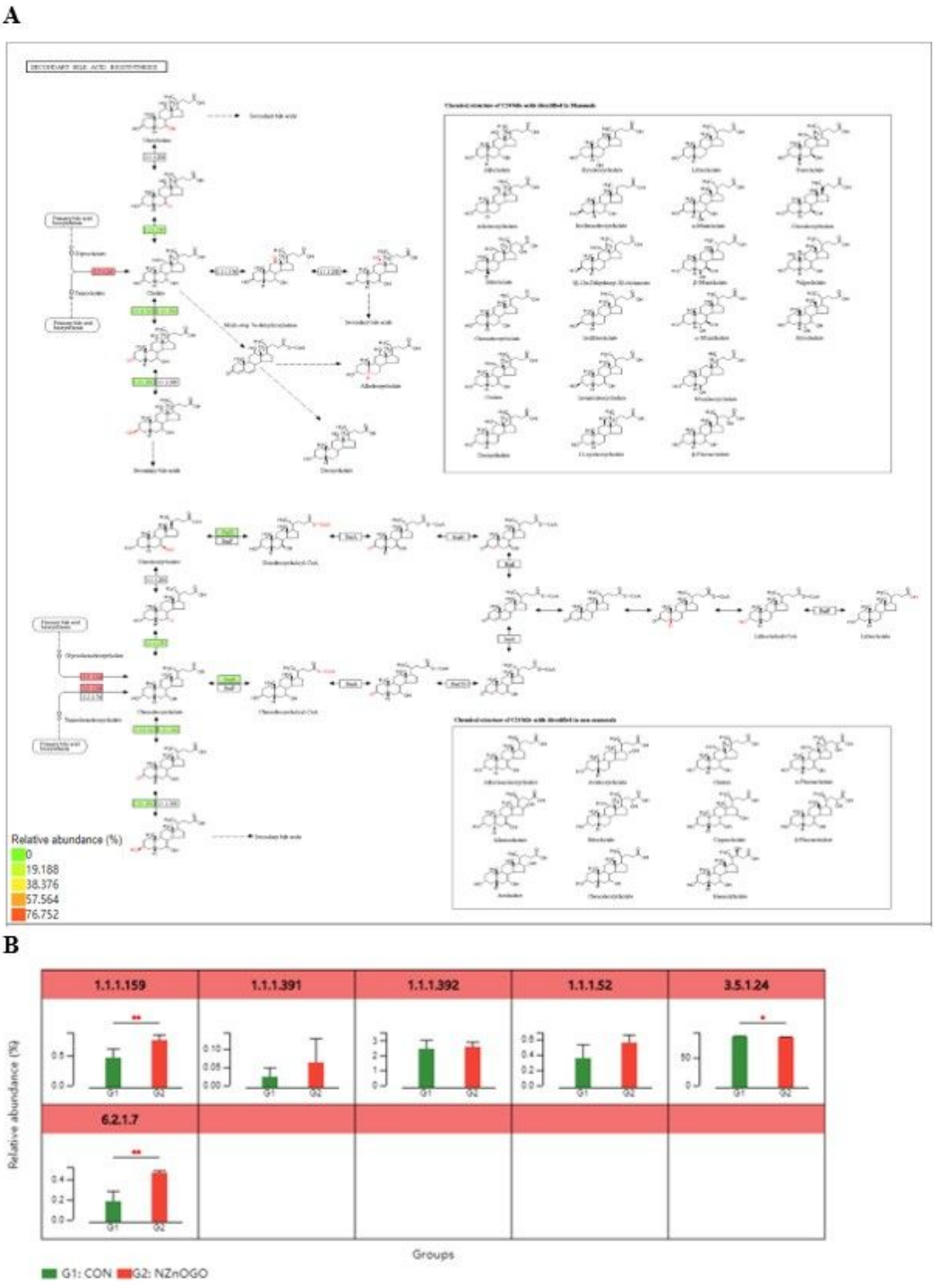

Figure 4

Secondary BA synthesis pathway analysis displaying the change between 2 groups. (A) differ secondary BA synthesis pathway, (B) differ enzyme. CON, control group; NZnOGO, graphene oxide loaded with NanoZnO group, BA = bile acid. Cattle were regarded as the experimental units, *n* = 5 for each group.

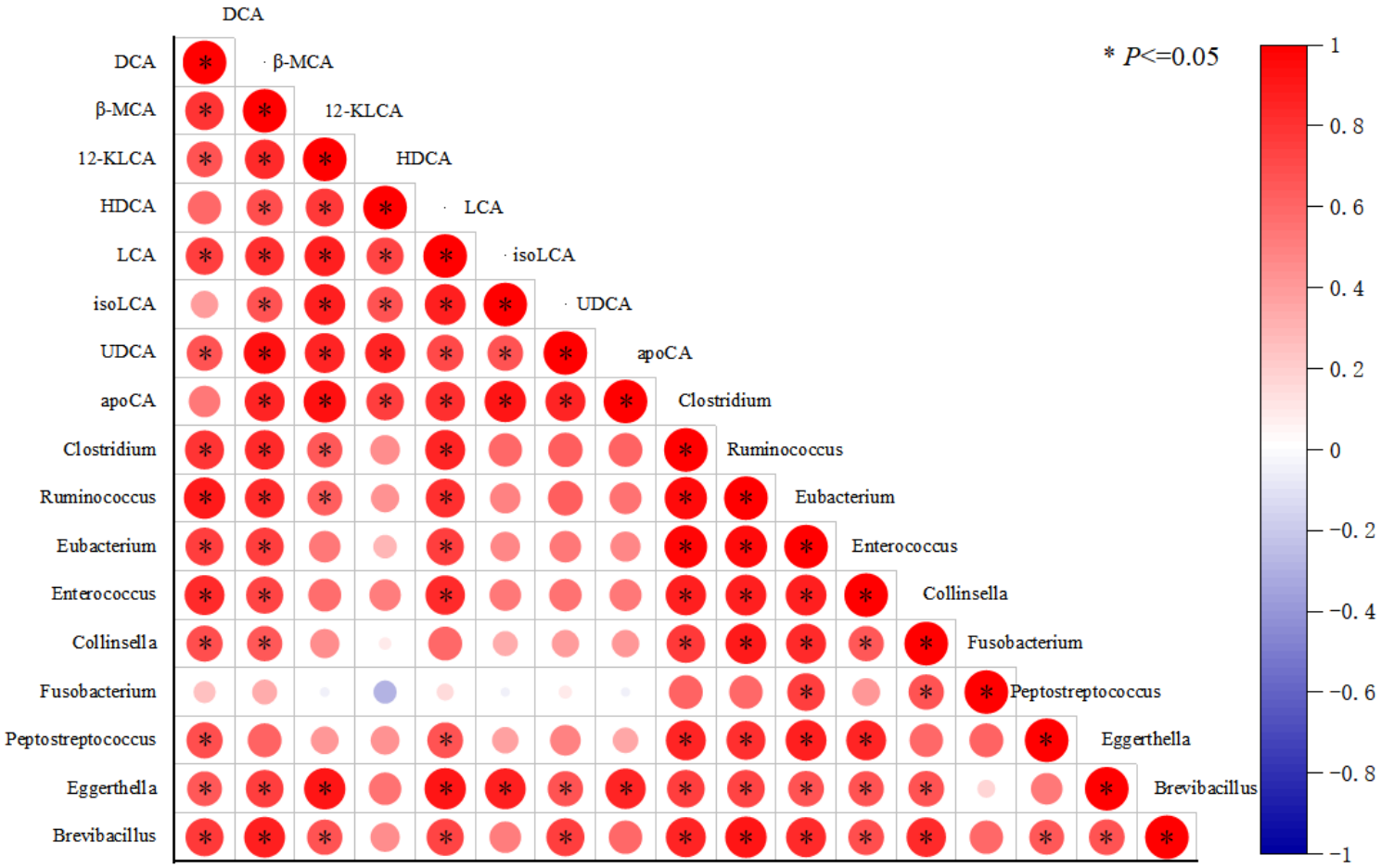

Figure 5

Pearson correlation analysis between secondary BA synthesis bacterial genera and secondary BA concentration of cattle fed the NZnOGO vs. CON diet. *Asterisks indicate significant correlations between genera and secondary BA concentrations. The positive correlation (closer to 1) for red and the negative correlation (closer to -1) for blue. CON, control group; NZnOGO, graphene oxide loaded with Nano-ZnO group; BA = bile acid. DCA = deoxycholic acid; β-MCA = beta-Muricholic acid; 12-KLCA = 12-ketolithocholic acid; HDCA = hyodeoxycholic acid; LCA = lithocholic acid; isoLCA = isolithocholic acid; UDCA = ursodeoxycholic acid; apoCA = apocholic acid. Cattle were regarded as the experimental units, *n* = 5 for each group.

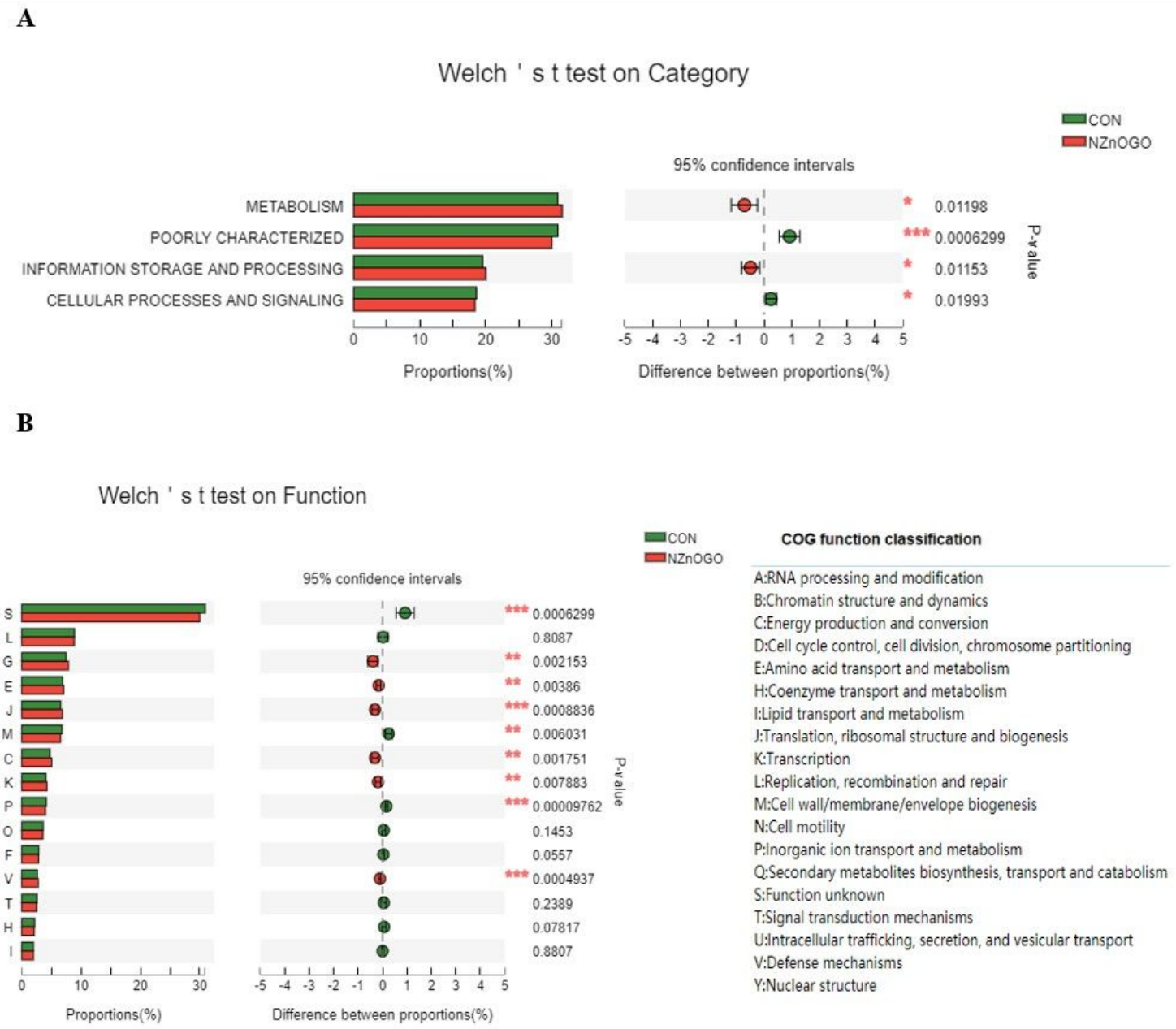

Figure 6

Clusters of Orthologous Groups of proteins (COGs) analysis displaying the change between 2 groups. (A) differ category, (B) differ function. CON, control group; NZnOGO, graphene oxide loaded with Nano-ZnO group. Cattle were regarded as the experimental units, *n* = 5 for each group.

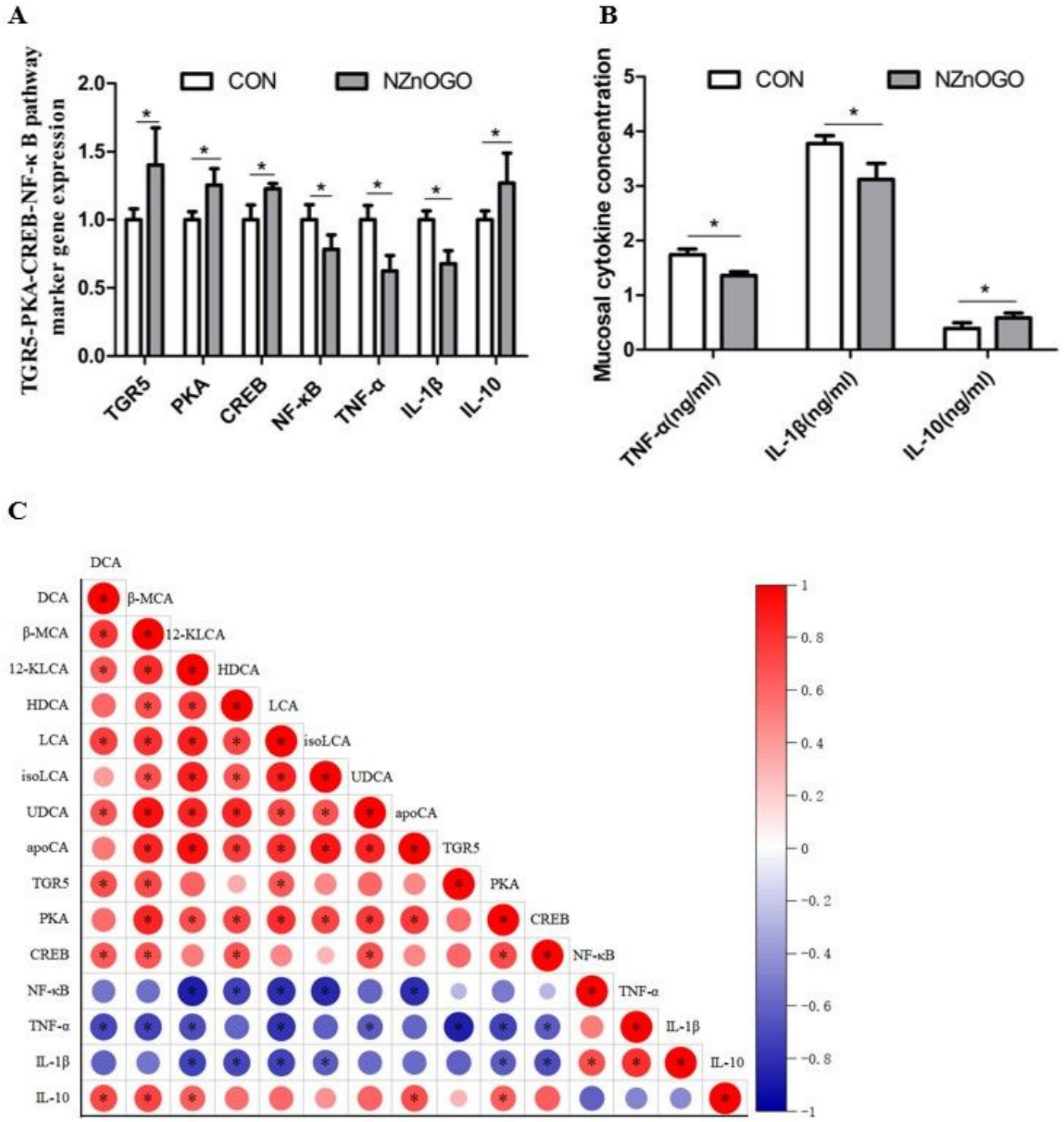

Figure 7

Effect of NZnOGO on intestinal immune function of cattle. (A) TGR5-PKA-CREB-NF-κB pathway marker gene expression, (B) Mucosal cytokine concentration in colon of cattle, (C) Pearson correlation analysis between secondary BA concentration and gene expression. Data are presented as means ± SD, *n* =5. Values with different *asterisks indicate significant (*P*<0.05). CON, control group; NZnOGO, graphene oxide loaded with Nano-ZnO group; BA, bile acid. TGR5 = Takeda G-protein-coupled receptor 5; PKA = protein kinase A; CREB = cyclic-AMP response element binding protein; NF-κB = nuclear factor kappa-B; TNF-α = tumor

necrosis factor-α; IL-1β = interleukin-1 β; IL-10 = interleukin-10; DCA = deoxycholic acid; β-MCA = beta-Muricholic acid; 12-KLCA = 12-ketolithocholic acid; HDCA = hyodeoxycholic acid; LCA = lithocholic acid; isoLCA = isolithocholic acid; UDCA = ursodeoxycholic acid; apoCA = apocholic acid.

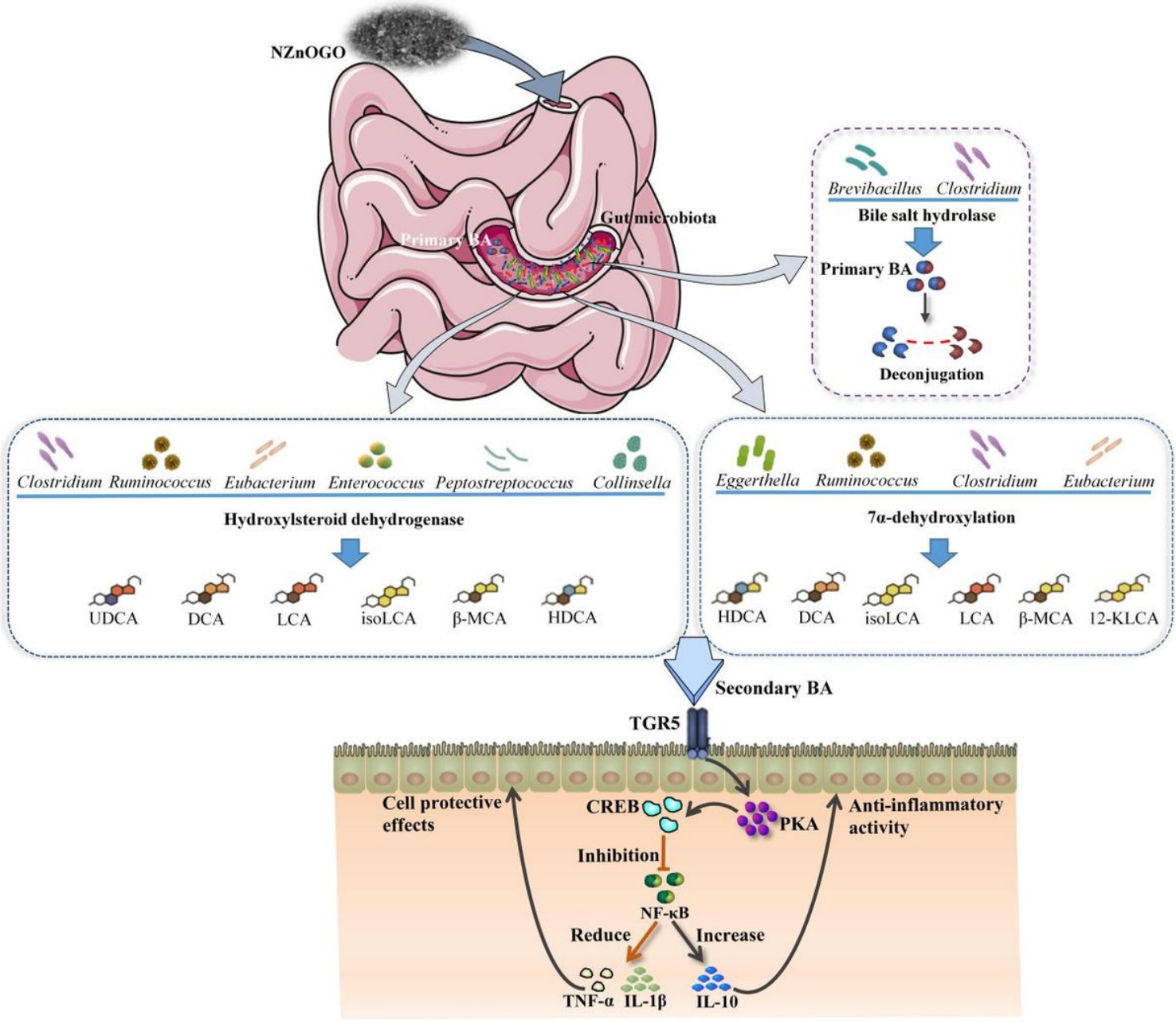

Figure 8

NZnOGO alters gut microbiota to promote secondary BA synthesis and potentiates intestinal immunity response in fattening cattle. NZnOGO = graphene oxide loaded with nano-ZnO group; BA = bile acid; UDCA = ursodeoxycholic acid; DCA = deoxycholic acid; LCA = lithocholic acid; isoLCA = isolithocholic acid; β-MCA = beta-Muricholic acid; HDCA = hyodeoxycholic acid; 12-KLCA = 12-ketolithocholic acid; TGR5 = Takeda G-protein-coupled receptor 5; PKA = protein kinase A; CREB = cyclic-AMP response element binding protein;

NF-κB = nuclear factor kappa-B; TNF-α = tumor necrosis factor-α; IL-1β = interleukin-1 β; IL-10 = interleukin-10.